Biochimica et Biophysica Acta 1793 (2009) 1656–1668

Contents lists available at ScienceDirect

Biochimica et Biophysica Acta

journal homepage: www.elsevier.com/locate/bbamcr

# Induction of glioma apoptosis by microglia-secreted molecules: The role of nitric oxide and cathepsin B

So-Young Hwang [a,1], Byong-Chul Yoo [b,1], Jae-won Jung [a], Eok-Soo Oh [c], Ji-Sun Hwang [a], Jin-A Shin [a], Song-Yi Kim [a], Seok-Ho Cha [a], Inn-Oc Han [a,*]

[a] Department of Physiology and Biophysics, and Center for Advanced Medical Education by BK21 Project, Inha University, College of Medicine, 253, Yonghyun-Dong, Nam-Ku, Incheon 402-751, Korea

[b] Research Institute, National Cancer Center, Goyang, Gyeonggi, Korea

[c] Department of Life Sciences, Division of Molecular Life Sciences and Center for Cell Signaling Research, Ewha Womans University, Seoul, Korea

ARTICLE INFO

*Article history:*
Received 9 February 2009
Received in revised form 12 August 2009
Accepted 28 August 2009
Available online 11 September 2009

*Keywords:*
Microglia
Glioma
Apoptosis

ABSTRACT

Microglia contributes significantly to brain tumor mass, particularly in astrocytic gliomas. Here, we examine the cytotoxic effects of soluble components secreted from microglia culture on glioma cells. Microglia conditioned culture medium (MCM) actively stimulated apoptotic death of glioma cells, and the effects of MCM prepared from LPS- or IFN-γ-activated microglia were more pronounced. The cytotoxic effects were glioma-specific in that primary cultured rat astrocytes were not affected by MCM. A donor of peroxynitrite induced glioma-specific cell death. In addition, NO synthase inhibitor suppressed glioma cell death induced by activated MCM, indicating that NO is one of the key molecules responsible for glioma cytotoxicity mediated by activated MCM. However, since unstimulated resting microglia produces low or very limited level of NO, MCM may contain other critical molecule(s) that induce glioma apoptosis. To identify the proteins secreted in MCM, proteomic analysis was performed on control or activated medium. Among over 200 protein spots detected by Coomassie blue staining, we identified 26 constitutive and 28 LPS- or IFN-γ-regulated MCM proteins. Several cathepsin proteases were markedly expressed, which were reduced upon activation. In particular, suppression of cathepsin B by the chemical inhibitors significantly reversed MCM-induced glioma cell death, implying a critical role of this protease in cytotoxicity. Our findings provide evidence on the functional implications of specific microglial-secreted proteins in glioma cytotoxicity, as well as a basis to develop a proteomic databank of both basal and activation-related proteins in microglia.



## 1. Introduction

Malignant gliomas are among the most fatal cancer types. In addition to neoplastic cells, the tumor microenvironment comprises nonmalignant cells, such as lymphocytes, astrocytes, endothelial cells, microglia, and macrophages, which influence cancer growth and therapeutic efficacy. Significant macrophage and microglia infiltration in both human and animal brain tumors has been consistently reported [1–4], and there is compelling evidence that microglia play an active role in glioma development [2,5]. However, the involvement of microglia in controlling the growth and infiltration of tumor cells remains a topic of controversy. Microglial cells are present in both the necrotic areas of brain tumor and intact tumor tissue of astrocytic gliomas, supporting a potential role in tumor promotion [6]. On the other hand, microglial secretory compounds may inhibit glioma development via suppression of glioma cell growth [7]. In this case, the biological success of glioma indicates that natural microglial defense mechanisms do not function properly. For example, glioma-infiltrating microglia's anti-tumor activity is limited by characteristic down-regulation of microglial peripheral benzodiazepine receptor. Microglial activity possibly depends on the type of tumor, immune status, or interactions with other cells in the brain.

Peroxynitrite, a highly reactive molecule formed by the near-diffusion reaction of nitric oxide (NO) and superoxide anion, is one of the most potent neurotoxic agents targeting both neurons and glial cells [8,9]. While astrocytes are relatively more resistant to oxidative injury than neurons due to the high level of intracellular oxidants, including glutathione [10], several investigators report that peroxynitrite exerts cytotoxic effects on astrocytes at submillimolar concentrations in cultured cells [11–13]. In contrast, several conflicting studies show that peroxynitrite displays cytoprotective effects depending on its concentration, cell type, and the oxidative states [14–16].

Proteomic analysis is one the most powerful methods for the identification of secretory proteins [17,18]. In the present study, we employed the proteomic approach to obtain an unbiased overview of the proteins secreted by microglia cultures. Notably, cathepsin proteins are abundant in the supernatant fractions of microglia culture. Accumulating evidence shows that intracellular and extracellular

* Corresponding author. Tel.: +82 32 890 0924; fax: +82 32 890 0647.
*E-mail address:* iohan@inha.ac.kr (I.-O. Han).

[1] Equally contributed to this work.

0167-4889/$ – see front matter © 2009 Elsevier B.V. All rights reserved.
doi:10.1016/j.bbamcr.2009.08.011

proteases of microglia contribute to various events in the central nervous system (CNS) through both nonspecific and limited proteolysis. Cathepsin B specifically exerts cytotoxic effects in the CNS. Microglia-secreted cathepsin B plays an important role in Aβ-induced neuronal apoptosis [19]. Moreover, in slice cultures from rodents and *in vivo* studies on primates, selective cathepsin B inhibitors protect against ischemia-induced neuronal damage [20], which is partly mediated by inflammatory and immunological reactions [21].

Here, we show that microglia induce apoptosis of glioma cells via the release of NO and cathepsin B protease. Our findings collectively indicate that the initiation or development of gliomas may be constitutively monitored by neighboring microglia cells via release of these factors, and breakdown of this balance is associated with tumor progression. Thus, effective regulation of microglia recruitment or activation may contribute to the successful therapeutic targeting of brain neoplasms.

## 2. Materials and methods

### 2.1. Reagents

Bacterial lipopolysaccharide (LPS), thrombin, propidium iodide (PI), 4′6-diamidino-2-phenylindole (DAPI), 3-morpholinosydnonimine (SIN-1), $N^G$-monomethyl-l-arginine (l-MMNA), 4-(2-aminoethyl) benzenesulfonylfluoride (AEBSF), *trans*-epoxysuccinyl-leucylamido (4-guanidino)butane (E-64), pepstatin, *N*-acetyl-L-leucyl-L-leucyl-L-norleucinal (LLnL), and cathepsin B were purchased from Sigma Chemical Company. CA-074me (Calbiochem) and Z-Val-Ala-Asp-FMK (zVAD-fmk) (Enzyme Systems Products) were obtained from local suppliers.

### 2.2. Cell cultures

The murine BV2 cell line has been used as a suitable model for *in vitro* studies of activated microglial cells [22]. It has been verified that the behavior of the BV2 microglial cell line closely mimics that of microglia cells in primary culture [22,23]. BV2 cells were maintained at 37 °C at 5% $CO_2$ in Dulbecco's modified Eagle's medium (DMEM) supplemented with 10% heat-inactivated endotoxin-free fetal bovine serum (FBS) (Hyclone), 2 mM glutamine, 100 μg/ml streptomycin, and 100 U/ml penicillin. U373-MG and U87-MG human glioma [24] and C6 rat glioma cell lines were cultured in DMEM medium and CRT-MG human glioma cells [25] were cultured in RPMI-1640 medium, each supplemented with 10% FBS, streptomycin, and penicillin.

### 2.3. Preparation of primary astrocytes and microglia

Primary microglia were prepared from 1-day-old Sprague Dawley rats as described previously, with some modifications [22]. In brief, animals were sacrificed by decapitation, the cerebral cortex was aseptically isolated, and the meninges were carefully removed. The tissue was dissociated in 0.25% trypsin in PBS. Cells were triturated into single cells in MEM containing 10% FBS, and plated on MEM supplemented with 2 mM L-glutamine, 33 mM glucose, 3 mM $NaHCO_3$, 10 mM HEPES, and 10% FBS for 10–14 days. To prepare microglia, cells were removed from the T75-flasks by mild shaking at 200 rpm for 2 h [26]. Enriched microglia were nearly pure (>95%), as evident from immunocytochemical staining for a microglia-specific marker, the CR3 complement receptor, detected using the OX-42 antibody (Roche Diagnostics). Astrocytes remaining in T75 flasks after removal of microglia were harvested with 0.1% trypsin. Astrocytes were subcultured twice to ensure sufficient purity for experiments. Astrocyte purity was confirmed by staining for specific glial fibrillary acidic protein (GFAP) (usually >99%). All experiments were carried out in accordance with "The Guidelines for Animal Research at Inha University School of Medicine".

### 2.4. Preparation of microglia conditioned culture medium

For conditioned medium transfer, primary cultured rat or BV2 mouse microglial cells were plated and either left untreated or stimulated with LPS, IFN-γ, or thrombin. Cell-free supernatant fractions were collected after 24–72 h of treatment, and applied to primary astrocytes or various glioma cell lines.

MCM for proteomic analysis was prepared as follows: cells were grown at $1.2\times10^7$/cells/140 $cm^2$, washed three times with PBS, and cultured in serum-free medium containing either LPS or IFN-γ. After 24 h, conditioned culture medium was collected by centrifugation, and passed through a 0.2 μm pore membrane filter (Millipore). Medium was concentrated with a centrifugal concentrator (Centriprep P-10; Millipore), and precipitated with 10% (v/v) TCA for 4 h at 4 °C. The pellet was washed with ethanol, and resuspended in urea buffer (7 M urea, 2 M thiourea, 40 mM Tris, 4% CHAPS, 0.5% carrier [Resolyte pH 3.5–10] ampholytes, 15 mM DTT, 1 mM EDTA, 1 mM PMSF, 2% protease inhibitor cocktail, 0.008% bromophenol blue) for 2-D (0.4 mg/gel) gel analysis.

### 2.5. Cell viability

Cells were grown in 24-well plates at a concentration of $5\times10^4$ cells/2 $cm^2$ followed by proper treatment. Morphological change was examined under the upright type phase-contrast microscopy (Olympus). Fifty microliters of 5 mg/ml 3-[4,5-dimethylthiazol-2-yl]-2,5-diphenyltetrasolium bromide (MTT) (Sigma-Aldrich) in growth medium were added to each well. After incubation for 4 h at 37 °C with MTT, cell medium was removed. The precipitated formazan, a product of MTT tetrazolium ring by the action of mitochondrial dehydrogenases, was solubilized with dimethyl sulfoxide and quantified spectrophotometrically at 540 nm.

### 2.6. Nitrite assay

NO production was determined by measuring the amount of nitrite, a relatively stable oxidation product of NO, as described previously [22]. In brief, an aliquot of the conditioned culture medium was mixed with an equal volume of 1% sulfanilamide in water and 0.1% *N*-1-naphthylethylenediamine dihydrochloride in 5% phosphoric acid. The absorbance was determined at 540 nm. Sodium nitrite was used to generate a standard curve.

### 2.7. Apoptosis assay by DAPI staining

DAPI staining was performed as reported previously [26], with some modifications. In brief, attached cells were washed with PBS, and fixed with 4% PBS-buffered paraformaldehyde solution for 30 min at RT. Fixing solution was removed, and cells were washed with PBS. Cells were treated with pure 0.5% Triton X-100 in PBS, and incubated for 15 min. Next, cells were rinsed with PBS for 5 min, and stained with 1 μg/ml DAPI in the dark for 30 min. Following rinsing with PBS and mounting on glass slides, at least 300 cells per condition were subjected to examination using a fluorescence photomicroscope (Carl Zeiss). Apoptotic cells were identified on the basis of morphology, as well as condensation and fragmentation of nuclei.

### 2.8. Flow cytometric analysis of the cell cycle

Cell cycle analysis was performed as reported previously [27], with some modifications. For cell cycle analysis, $1\times10^6$ BV2 cells were washed twice with PBS. Cells were fixed with 70% ethanol at −20 °C for at least 12 h. After two washes with PBS, cells were incubated in RNase A/PBS (100 μg/ml) at 37 °C for 30 min. Intracellular DNA was labeled with PI (50 μg/ml) for 30 min on ice protected from light, and analyzed with a FACSCalibur fluorescence-activated cell sorter (FACS) (Becton Dickinson).

### 2.9. Immunoblotting

Prepared cells were resuspended in lysis buffer (10 mM Tris, 140 mM NaCl, 1% Triton, 0.5% SDS, and protease inhibitors, pH 8.0) and cleared from cellular debris by centrifugation. Protein samples (20 μg for regular Western and 40 μg for 2-D Western blotting) were separated by SDS–PAGE and transferred to Hybond™-ECL™ membrane (Amersham Biosciences). The membrane was blocked with 5% BSA in TBST solution (10 mM Tris–HCl, pH 8.0, containing 150 mM NaCl and 0.5% Tween 20). Blots were incubated with human PARP (BD Pharmingen), iNOS (BD Pharmingen), apolipoprotein E (Santa Cruz Biotechnology), cathepsin A (R&D Systems), cathepsin B (Abcam), cathepsin D (Abcam), cathepsin L (R&D Systems), or HSP60 (Abcam). Membranes were washed, incubated with diluted HRP-conjugated secondary antibodies (Amersham Biosciences), and developed by the enhanced chemiluminescence (ECL) detection system (Amersham Biosciences).

### 2.10. 2-D image analysis and MALDI-MS

2-D of prepared MCM and MALDI-MS analysis were performed as reported previously, with some modifications [28]. In brief, 400 mg of secreted protein were applied to a 13 cm immobilized nonlinear gradient strip (pH 3–10) (Amersham Biosciences), and focused at 8000 V within 3 h. Second-dimension separation was performed using 12% polyacrylamide gels (chemicals from Serva and Bio-Rad). 2-D gels were stained with colloidal Coomassie blue (Invitrogen) or silver nitrate for 24 h, and destained with deionized water. ImageMaster™ software (Amersham Biosciences) was applied for image analysis of 2-D gels. Protein spots in control MCM and those displaying altered secretion patterns in the presence of LPS or IFN-γ were subjected to MALDI-MS for identification.

For MALDI-MS analysis, protein spots in 2-D gels were excised, destained with 50% acetonitrile in 0.1 M ammonium bicarbonate, and dried in a Speedvac evaporator. Dried gel pieces were reswollen with 30 μl of 25 mM sodium bicarbonate, pH 8.8, containing 50 ng trypsin (Promega, Madison) at 37 °C overnight. α-Cyano 4 hydroxycinnamic acid (Bruker Daltonics) (20 mg) was dissolved in 1 ml acetone: ethanol (1:2, v/v), and 0.5 μl matrix solution was mixed with an equivalent volume of sample. The sample was analyzed using an Ultraflex TOF/TOF system (Bruker Daltonics). Peptide masses were matched with the theoretical peptide masses of proteins from all species in the Mascot database.

### 2.11. Statistical analysis

Data are expressed as means ± SEM, and analyzed for statistical significance using analysis of variance (ANOVA) followed by Scheffe's test for multiple comparison. A $p$ value of $<0.05$ was considered significant.

## 3. Results

### 3.1. Microglia conditioned culture medium (MCM) decreases glioma cell viability and activated MCM is more potent in inducing glioma cell death

We investigated the effects of BV2 microglia conditioned culture medium (MCM) on proliferation or survival of astrocytes and glioma. Conditioned culture media prepared from primary cultured rat microglia or murine BV2 cell line were incubated with rat primary astrocytes or CRT-MG human astrocytic glioma cells. Cell viability was measured with the MTT assay at 72 h. Transfer of MCM prepared from BV2 or primary microglia markedly reduced the viability of CRT-MG cells. In contrast, astrocytes were not significantly influenced by MCM (Fig. 1A). Rather, MCM consistently induced low-level proliferation of astrocytes (Figs. 1A and C and 2F). We additionally examined cell status and morphological changes after MCM treatment (Fig. 1B). Incubation of astrocytes or CRT-MG cells with MCM of BV2 and primary cultured rat microglial cells for 72 h triggered a dramatic decrease in glioma numbers and morphological changes into elongated shape followed by detaching from plates but no significant changes of astrocytes in terms of both cell number and phenotype.

To determine the influence of MCM prepared from activated microglia, BV2 cells were treated with the well-characterized immune stimulants bacterial lipopolysaccharide (LPS), thrombin, or IFN-γ [22,23,29], followed by collection of MCM. MCM consistently exerted cytotoxic effects on CRT-MG cells. Moreover, LPS-stimulated MCM of BV2 or primary microglia had a more potent effect in a dose-dependent manner (Fig. 1C and Suppl. Fig. 1). In comparison, astrocytes were not influenced by MCM, and minimally affected by activated MCM. LPS, administered directly at equivalent doses, did not affect cell viability or proliferation of CRT-MG or astrocytes. The influences of residual LPS in activated MCM were tested. Co-treatment with LPS (1, 5, or 10 ng/ml) and MCM did not significantly change the cytotoxic effects of MCM alone (Suppl. Fig. 2).

Activated MCM prepared from LPS-, thrombin-, or IFN-γ-stimulated BV2 cells exerted potent cytotoxic effects on CRT-MG survival to a similar extent (data not shown). Next, we examined the effects of MCM and activated MCM on several other rat (C6) or human (U87-MG and U373-MG) glioma cell lines. As expected, MCM induced cytotoxicity in C6, U87-MG, and U373-MG cells and activated MCM (Fig. 1D) exerted more significant cytotoxicity, indicating that these effects on glioma cells are general rather than cell type-specific.

### 3.2. MCM and activated MCM trigger apoptosis of glioma cells

Cells were then subjected to DAPI staining, which revealed chromatin condensation, a hallmark of apoptosis. Incubation of CRT-MG with MCM showed condensed nuclei, and incubation with activated MCM gave rise to condensed nuclei with evidence of DNA fragmentation (Fig. 2A). MCM and activated MCM prepared from rat primary microglia also induced nuclei condensation and DNA fragmentation in CRT-MG cells (data not shown). This apoptotic characteristic was confirmed by cell cycle analysis. Cells were treated with propidium iodide and the percent of sub-G1 phase, characterized as fragmented DNA, was determined by FACS analysis. Treatment of MCM resulted in 9.54% of cells entering the sub-G1 phase, which is an indicator of apoptosis, and this proportion increased to 22.72% for cells treated with activated MCM (Fig. 2B). Moreover, PARP cleavage, the final stage marker of apoptosis, was observed at 24 h in BV2 cells and rat primary microglia incubated with MCM or activated MCM (Fig. 2C).

To further verify MCM-induced apoptotic death, we treated the MCM-treated CRT-MG glioma cells with the general apoptosis inhibitor zVAD-fmk and examined whether the apoptosis was blocked. zVAD-fmk (1, 10, or 100 μM) was incubated with or without MCM to treat glioma cells. Observing under a light microscope, MCM-induced cell death was almost completely blocked by zVAD-fmk (Fig. 2D). While zVAD-fmk itself exerted dose-dependent cytotoxicity (about 15% cell death at 10 μM), MCM-triggered apoptosis was significantly suppressed, as measured with the MTT assay (Fig. 2E). However, zVAD-fmk alone had no significant effects on astrocytes and MCM-treated astrocytes (Fig. 2F). zVAD-fmk (10 μM) also suppressed cytotoxicity induced by MCM of rat primary microglia (Suppl. Fig. 3).

### 3.3. NO influences glioma cell death

3-Morpholinosydnonimine (SIN-1) is a potent exogenous donor of peroxynitrite, a highly reactive molecule formed from NO in aqueous solutions [30]. Treatment of astrocytes or the glioma subconfluent monolayer with SIN-1 (0–1000 μM) for 72 h induced nitric oxide in a

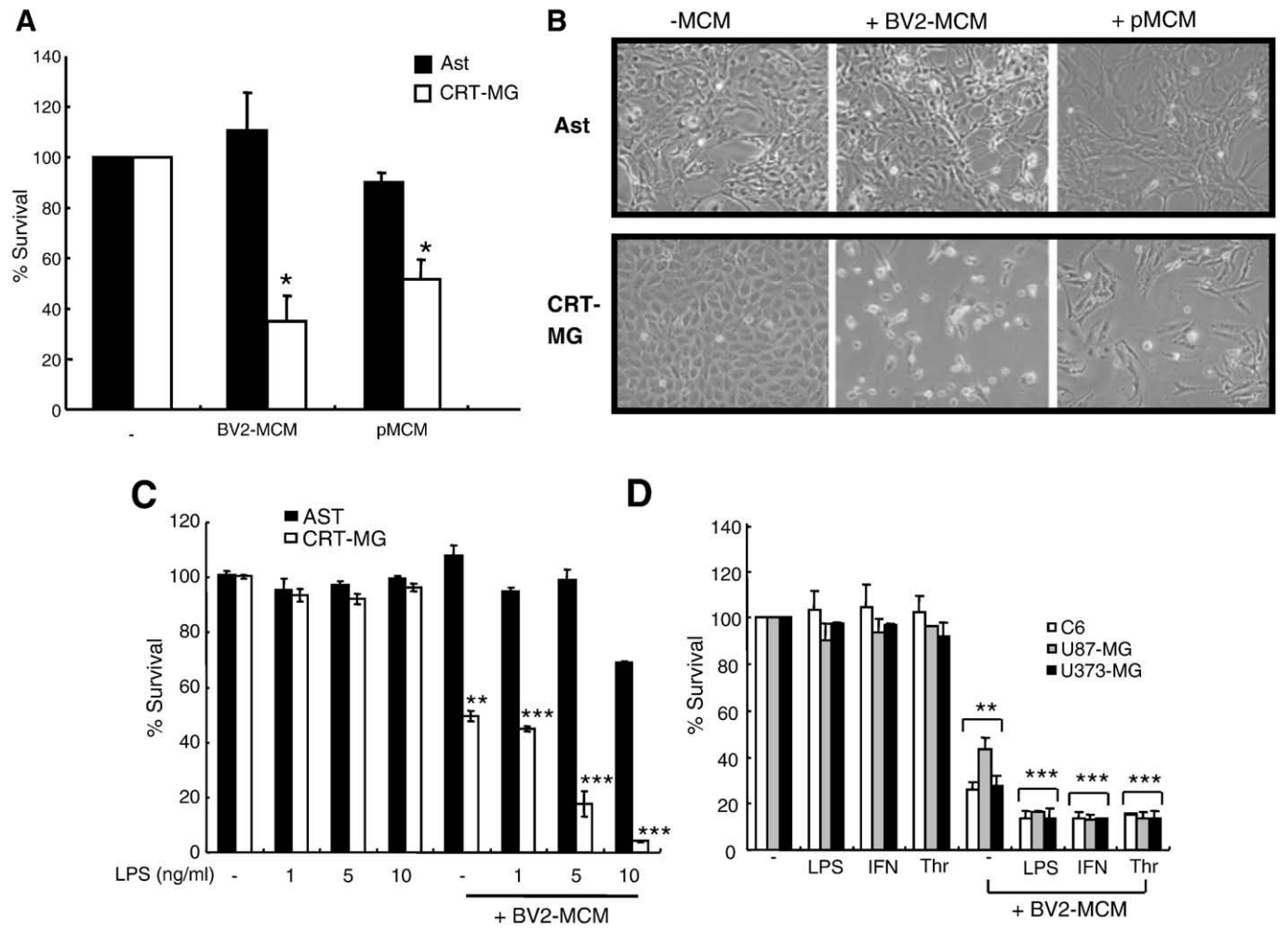


**Fig. 1.** Induction of CRT-MG glioma cell death by MCM and MCM prepared from activated microglia. (A and B) Conditioned media of unstimulated BV2 (BV2-MCM) or rat primary microglia (pMCM) were prepared and incubated with astrocytes (Ast) or CRT-MG glioma cells for 72 h. (A) Cell survival was determined using the MTT assay. (B) Cell status and morphology were observed using phase-contrast light microscopy. (C) BV2 cells were left untreated or stimulated with 1, 5, or 10 ng/ml of LPS for 24 h. MCM prepared from control and activated BV2 cells was incubated with astrocytes or CRT-MG cells. As a control, equivalent doses of LPS were added directly to astrocytes and CRT-MG cells. Cell viability was measured at 72 h using the MTT assay. (D) BV2 cells were left untreated or stimulated with LPS (100 ng/ml), IFN-γ (IFN) (20 U/ml), or thrombin (Thr) (50 U/ml). BV2-MCM was collected 24 h later, and incubated with C6 rat glioma and U87-MG and U373-MG human glioma cells for 72 h. Glioma cells treated directly with LPS (100 ng/ml), IFN-γ (20 U/ml), or thrombin (50 U/ml) were used as control cultures. Cell viability was measured using the MTT assay. Bars represent means ± SEM of three independent experiments. * represents values significantly decreased in BV2-MCM or pMCM, compared to control cultures. ** indicates values significantly decreased by MCM, compared to control cultures. *** represents values that differ significantly between activated MCM and MCM.

dose-dependent manner (Fig. 3A). MTT and phenotypic results show that at these doses, SIN-1 does not significantly affect the cell viability of astrocytes (Fig. 3B, phenotypic data not shown). In contrast, SIN-1 mediated cytotoxic effects in CRT-MG glioma cells at concentrations higher than 200 μM (Fig. 3B) in a dose-dependent manner. Next, the effects of [$N^G$-monomethyl-l-arginine(l-NMMA)], a NOS-specific inhibitor, were examined (Fig. 3C). After BV2 cells were stimulated with LPS with or without NMMA, MCM was prepared and applied to CRT-MG cells. Specifically, only glioma cell death by activated MCM was significantly suppressed in the presence of NMMA. The data clearly suggest that NO released by activated microglia plays a major role in glioma cytotoxicity.

Not only do activated microglia exhibit increased production of NO, they also produce increased levels of proinflammatory cytokines and chemokines. It has been suggested that microglia represent the first line of CNS defense against brain tumors by virtue of the cytotoxic potential of the proinflammatory cytokines, IL-1, IL-6, IL-10, TNF-α, and/or TGF-β [5]. In our supplementary experiments, we examined the effects of proinflammatory cytokines on glioma cell fate and found that treatment with cytokines, such as IL-1β, TNF-α, or IL-6, did not affect the viability of CRT-MG cells (Suppl. Fig. 4A). Combined treatment with IL-1β, TNF-α, and IL-6 induced a modest decrease in cell viability, but significantly potentiated SIN-1-induced (100 and 200 μM) cytotoxicity (Suppl. Fig. 4B).

### *3.4. 2-D mapping to identify proteins secreted from BV2 for altered secretion patterns in the presence of LPS or IFN-γ and validation of 2-D mapping results by Western blotting*

In order to identify proteins in MCM, microglial proteins secreted from non-treated control MCM and that stimulated by LPS or IFN-γ were separated on the basis of their own pI and molecular weight (MW) on a 2-D gel. MCM was collected, concentrated, precipitated with TCA, and subjected to 2-D gel electrophoresis (0.4 mg/gel). After colloidal Coomassie blue staining, over 200 protein spots were detectable on each 2-D gel. Protein spots that displayed altered secretion patterns in the presence of LPS and IFN-γ were selected using image analysis software, and subjected to MALDI-MS analysis. Some spots could not be characterized with MALDI-TOF due to insufficiencies or overlap. In total, 54 protein spots were identified (Table 1). Swiss-Prot numbers of proteins displaying increased or decreased secretion following treatment with LPS and IFN-γ are

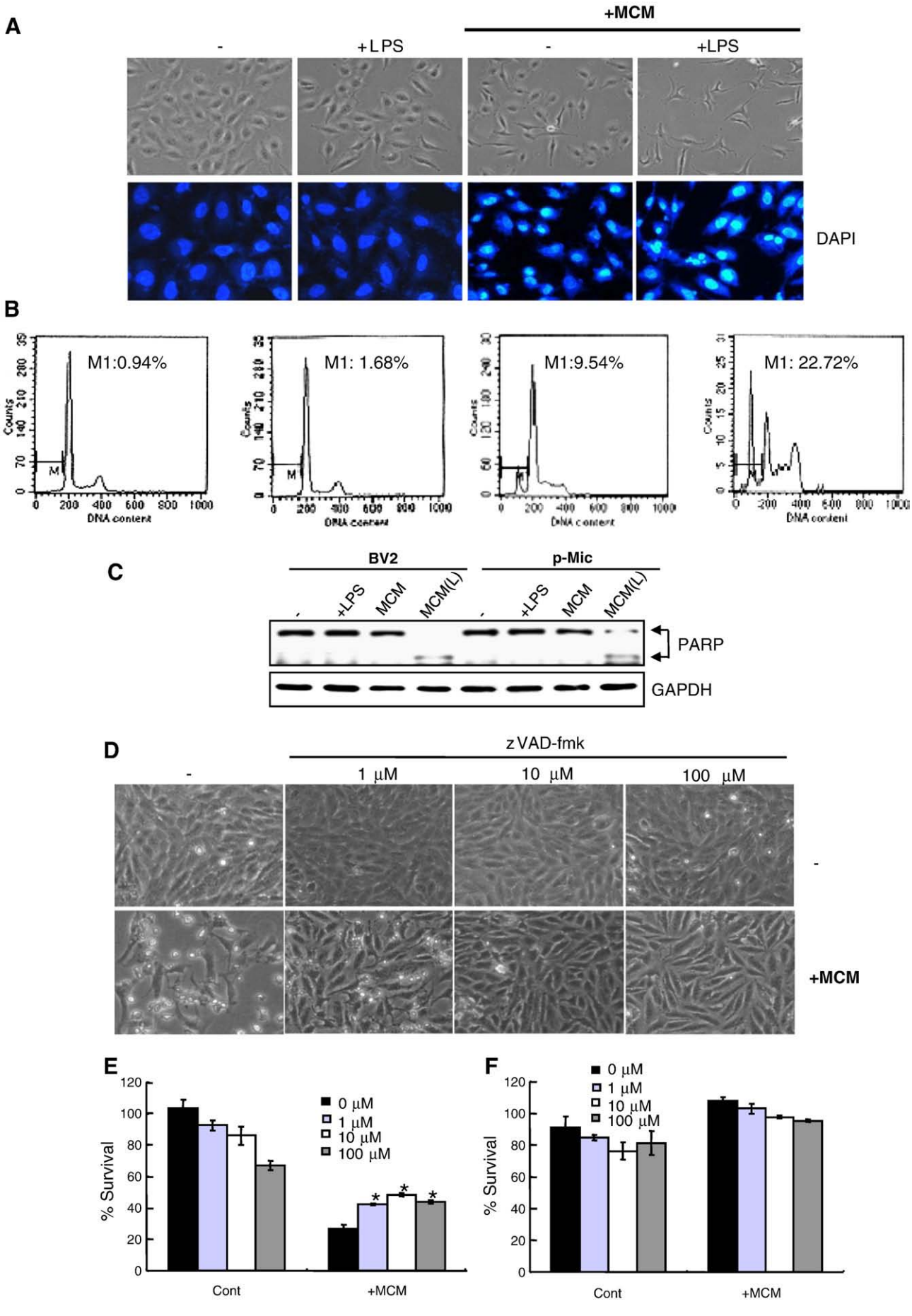
A
+MCM
-
+LPS
-
+LPS
DAPI
B
M1:0.94%
M1: 1.68%
M1:9.54%
M1: 22.72%
Counts
DNA content
C
BV2
p-Mic
-
+LPS
MCM
MCM(L)
-
+LPS
MCM
MCM(L)
PARP
GAPDH
D
zVAD-fmk
-
1 μM
10 μM
100 μM
-
+MCM
E
% Survival
0 μM
1 μM
10 μM
100 μM
Cont
+MCM
F
% Survival
0 μM
1 μM
10 μM
100 μM
Cont
+MCM

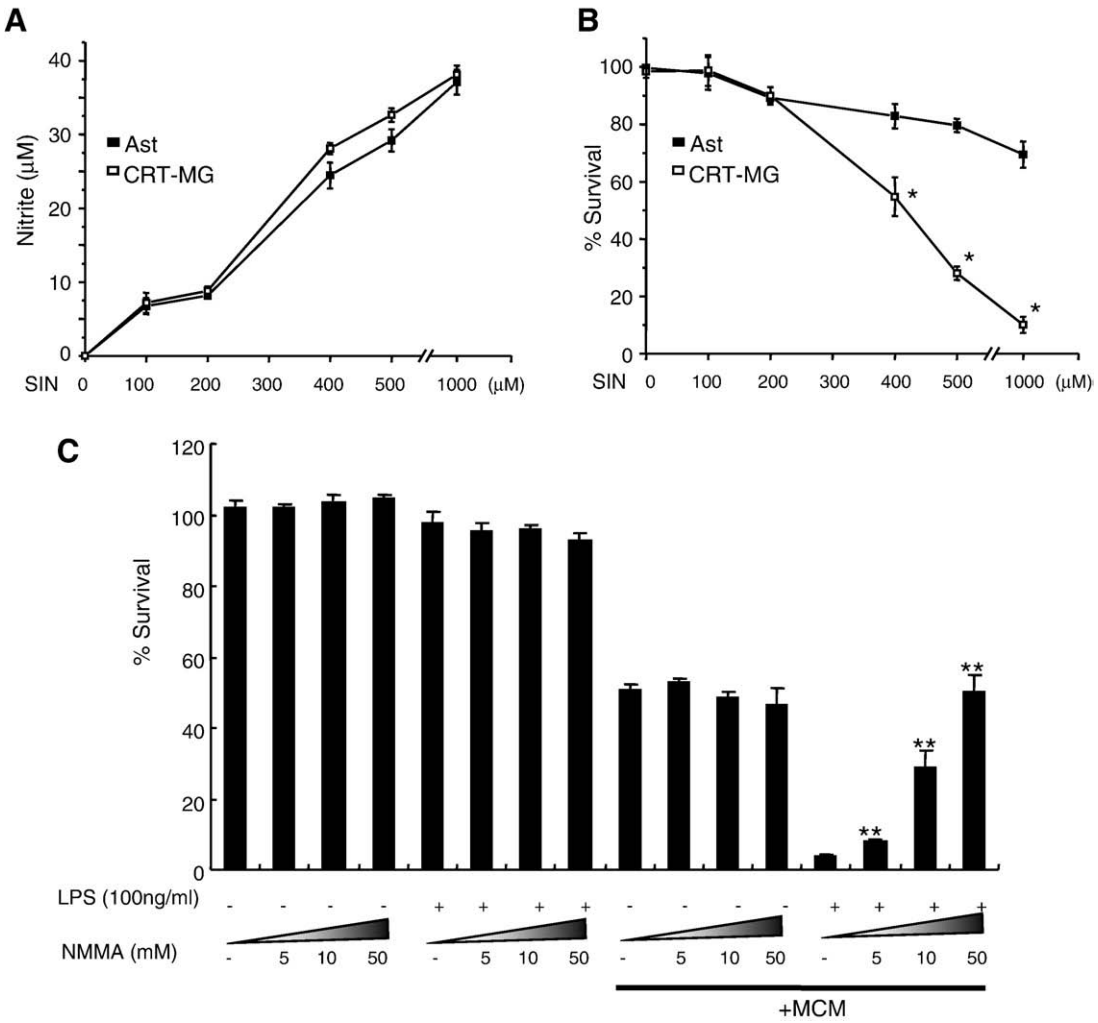


**Fig. 3.** The influence of SIN or NMMA on glioma cell death. Primary astrocytes or CRT-MG glioma cells were treated with different concentrations of SIN-1 (0, 100, 200, 400, 500, or 1000 μM) for 72 h. (A) Nitric oxide production was evaluated by measuring nitrite in the culture medium. (B) Cell survival was determined with the MTT assay. (C) BV2 cells were left untreated or pretreated with increasing concentrations of NMMA for 1 h before application of LPS (100 ng/ml). Cell-free conditioned culture medium was collected 24 h later, and incubated with the CRT-MG human glioma cell line for 72 h. As a control, equivalent doses of LPS and NMMA were added directly to CRT-MG cells. Survival rates of primary astrocytes and CRT-MG glioma cells were determined with the MTT assay. Bars represent means ± SEM of three independent experiments. * Indicates values significantly different from untreated control cultures. ** Indicates values significantly increased compared to control cultures incubated with activated MCM.

labeled in red or blue, respectively (Fig. 4A). Fig. 4B presents image analysis-based selection of apolipoprotein E (ApoE) (AAA37251) and cathepsin L (P06797) precursors as proteins displaying down-regulated secretion in the presence of LPS and IFN-γ. The majority of secreted proteins were not altered in the presence of LPS and IFN-γ (Fig. 4A). Among these proteins, 33 were identified to indicate landmark proteins and normalize the level of protein secretion (Table 1). The differential expression of a subset of identified proteins, such as ApoE, cathepsin L, and other cathepsin family proteases, was validated by Western blot analysis. Prior to Western blotting, silver staining of a SDS–PAGE gel was performed to detect protein patterns and confirm equivalent amounts of secreted protein (Suppl. Fig. 5). 2-D Western blotting for ApoE confirmed the presence of several subtypes or modified forms of ApoE proteins in MCM. Moreover, their levels were reduced in MCM preparations from LPS- or IFN-γ-stimulated microglia (Fig. 4C). In contrast, the ApoE mRNA level was not affected by LPS or IFN-γ (Suppl. Fig. 6). ApoE and cathepsin L, A, B, and D protein levels were evaluated by Western blotting. Decreased secretion was observed in the presence of LPS and IFN-γ (Fig. 4D). Notably, these proteins were not detected in whole cell lysates, suggesting that they are truly secretory proteins. The decrease in the cathepsin L, B, and D proteins level as a result of LPS and IFN-γ treatment was additionally confirmed in primary microglial cells (Suppl. Fig. 7). HSP60 was strongly detected in whole cell lysates, compared to the low level

**Fig. 2.** Induction of glioma cell apoptosis by MCM and activated MCM. (A–C) BV2 microglia cells or rat primary microglia were left untreated or stimulated with LPS (100 ng/ml) for 24 h. Cell-free conditioned culture medium {MCM for untreated and MCM(L) for LPS stimulated} was collected, and incubated with CRT-MG human glioma cells for a further 24 h. CRT-MG cells treated with LPS (100 ng/ml) were employed as control cultures. (A) Cell status and morphological changes in CRT-MG glioma cells were observed under a light microscope (upper panel). Cells were stained with DAPI and analyzed by fluorescence microscopy (lower panel). (B) Cell cycle analysis was performed after labeling intracellular DNA with propidium iodide, followed by FACS analysis at 24 h. The sub-G1 peak, marked as M1, indicates fragmented DNA. (C) Total cell lysates were prepared and PARP cleavage and GAPDH were detected on a Western blot. Data in (C) are representative of three separate experiments. (D) CRT-MG glioma cells were treated with or without MCM and the indicated concentrations of zVAD-fmk for 72 h. The morphology of CRT-MG glioma cells was observed under a light microscope. Shown data are representative of three independent experiments. (E and F) CRT-MG glioma cells (E) or rat astrocyte cells (F) were treated with or without MCM and the indicated concentrations of zVAD-fmk for 72 h. Cell survival rates were determined with the MTT assay. Data are means ± SEM of three independent experiments. * Indicates values significantly increased compared to cultures incubated with MCM.

**Table 1**
Identification of secretory proteins obtained from BV2.

| Protein accession number | | Full name of protein | Theoretical | | MALDI-MS | |
|---|---|---|---|---|---|---|
| | | | $M_r$ | pI | Peptide matched | Sequence coverage (%) |
| Landmarks | Q9ES94 | Cathepsin Z | 34,837 | 6.13 | 13 | 33 |
| | JC1224 | Nucleobindin precursor | 52,965 | 4.99 | 20 | 41 |
| | A45935 | DnaK-type molecular chaperone hsc70 | 71,021 | 5.37 | 41 | 55 |
| | S25197 | Transitional endoplasmic reticulum ATPase | 89,936 | 5.14 | 22 | 38 |
| | P58252 | Elongation factor 2 (EF-2) | 96,091 | 6.42 | 37 | 41 |
| | Q9CZW9 | 5-Aminoimidazole-4-carboxamide ribonucleotide formyltransferase | 62,351 | 6.65 | 23 | 33 |
| | Q99LF6 | Protein disulfide isomerase associated 3 | 57,099 | 5.88 | 27 | 60 |
| | BAC35834 | Unnamed protein product | 57,783 | 5.97 | 24 | 60 |
| | P05064 | Fructose-bisphosphate aldolase A | 39,787 | 8.31 | 19 | 71 |
| | S74227 | Cathepsin K (EC 3.4.22.-) precursor | 37,100 | 8.62 | 16 | 36 |
| | P63260 | Actin, cytoplasmic 2 (Gamma-actin) | 42,108 | 5.31 | 23 | 60 |
| | S06763 | Calreticulin precursor | 48,136 | 4.33 | 20 | 50 |
| | Q8C530 | Rab GDP dissociation inhibitor beta (Rab GDI beta) | | 5.93 | 28 | 57 |
| | P97324 | Glucose-6-phosphate 1-dehydrogenase 2 (EC 1.1.1.49) (G6PD). | 59,550 | 6.07 | 35 | 60 |
| | P17182 | Alpha-enolase (EC 4.2.1.11) | 47,322 | 6.36 | 27 | 62 |
| | Q9CXW3 | Calcyclin-binding protein (CacyBP) (Siah-interacting protein) | 26,608 | 7.63 | 14 | 48 |
| | P09411 | Phosphoglycerate kinase 1 (EC 2.7.2.3) | 44,700 | 7.52 | 18 | 51 |
| | Q9DBJ1 | Phosphoglycerate mutase 1 (EC 5.4.2.1) | 28,700 | 6.75 | 17 | 47 |
| | Q99LB4 | Capg protein | 39,030 | 6.47 | 13 | 45 |
| | P52480 | Pyruvate kinase isozyme M2 (EC 2.7.1.40) | 58,289 | 7.42 | 25 | 45 |
| | Q8BQV9 | 5-Aminoimidazole-4-carboxamide ribonucleotide formyltransferase | 37,854 | 5.65 | 19 | 56 |
| | P68143 | Actin, cytoplasmic 1 (beta-actin) | 42,000 | 5.29 | 28 | 70 |
| | Q8BK18 | Aspartyl-tRNA synthetase (EC 6.1.1.12) | 57,567 | 6.16 | 16 | 38 |
| | Q9JHU9 | Myo-inositol 1-phosphate synthase A1 (EC 5.5.1.4) | 61,520 | 5.99 | 12 | 28 |
| | P18242 | Cathepsin D precursor | 45,381 | 6.71 | 12 | 36 |
| | P08709 | Peroxiredoxin-6 | 24,938 | 5.72 | 9 | 46 |
| Down-regulated proteins in LPS- or IFN-γ-treated BV2 | BAC36723 | Unnamed protein product | 40,063 | 9.36 | 14 | 44 |
| | AAA37251 | Apolipoprotein E precursor | 35,901 | 5.56 | 24 | 49 |
| | AAL34533 | Transferrin | 78,794 | 6.92 | 29 | 36 |
| | P06797 | Cathepsin L precursor | 38,075 | 6.37 | 25 | 75 |
| | AAD54617 | Lysyl hydroxylase 1 | 84,113 | 6.08 | 31 | 43 |
| | Q8CFJ4 | Ariadne ubiquitin-conjugating enzyme E2 binding protein homolog 1 | 54,382 | 7.65 | 11 | 24 |
| Up-regulated proteins in IFN-γ-treated BV2 | Q8C2C7 | Heat shock protein, 60 kDa | 60,956 | 5.67 | 23 | 51 |
| | C25437 | Tubulin beta-3 chain | 50,255 | 4.79 | 27 | 48 |
| | Q9D2D1 | Protective protein for beta-galactosidase | 54,423 | 5.56 | 24 | 28 |
| | P09103 | Protein disulfide isomerase precursor | 57,422 | 4.79 | 28 | 54 |
| | BAB23644 | Unnamed protein product | 53,376 | 4.99 | 28 | 50 |
| | S43061 | T-complex-type molecular chaperone Ccte | 60,042 | 5.72 | 40 | 61 |
| | Q923D2 | Flavin reductase (FR) (NADPH-dependent diaphorase) | 22,297 | 6.49 | 12 | 74 |
| | A48513 | Macrophage 23K stress-induced protein | 22,390 | 8.26 | 21 | 52 |
| | BAB23595 | Unnamed protein product | 22,379 | 5.68 | 10 | 51 |
| | I57010 | Purine-nucleoside phosphorylase (EC 2.4.2.1) | 32,541 | 5.78 | 21 | 55 |
| | I58195 | Y box-binding protein 1 | 35,723 | 9.98 | 13 | 47 |
| | P11499 | HSP 90-beta (Tumor-specific transplantation 84 kDa antigen) (TSTA) | 83,484 | 4.97 | 31 | 43 |
| | S28182 | Lamin A | 74,482 | 6.41 | 16 | 32 |
| | Q922R8 | Protein disulfide isomerase A6 precursor | 48,100 | 5.00 | 17 | 31 |
| Up-regulated proteins in LPS-treated BV2 | AAF14001 | Scavenger receptor type A SR-A | 50,707 | 6.48 | 22 | 39 |
| | Q99KQ4 | Nicotinamide phosphoribosyltransferase | 55,698 | 6.69 | 21 | 57 |
| | AAH57565 | Tyki protein | 47,301 | 5.98 | 19 | 36 |
| | Q9JII6 | Alcohol dehydrogenase [NADP+] (EC 1.1.1.2) | 36,661 | 6.87 | 17 | 42 |
| | AK049817 | Purine-nucleoside phosphorylase | 32,527 | 5.78 | 15 | 54 |
| | Q9CWE7 | Triosephosphate isomerase | 27,109 | 6.90 | 10 | 35 |
| | AAH89335 | Vimentin | 53,712 | 5.06 | 24 | 60 |
| | C25437 | Tubulin beta-3 chain | 50,255 | 4.79 | 27 | 48 |

detected in the secretory proteins (Fig. 4D). Ponceau staining and HSP60 immunoblotting revealed equivalent amounts of secretory and whole cell lysate proteins (Fig. 4D).

### *3.5. Protease inhibitors, AEBSF, E-64, and LLnL, suppress microglia activation, and E-64 partially reverses MCM-induced cell death*

We examined the effects of proteases on microglia behavior, and consequently, glioma cell death. The effects of a general serine protease inhibitor {4-(2-aminoethyl)benzenesulfonylfluoride (AEBSF)}, a cysteine protease inhibitor [31], a cathepsin D inhibitor (pepstatin A), and a proteasome inhibitor {*N*-acetyl-L-leucyl-L-leucyl-L-norleucinal (LLnL)} on both microglia activation and MCM-induced glioma cell death were evaluated. Pretreatment of BV2 cells with AEBSF, E-64, or LLnL led to strong inhibition of mRNA induction of proinflammatory molecules, such as COX-2, IL-1β, TNF-α, and IL-6, as well as iNOS (Fig. 5A). Consistent with this, AEBSF, E-64, and LLnL suppressed iNOS protein expression in BV2 cells (Fig. 5B). The effects of AEBSF were further confirmed by suppression of NO release in a dose-dependent manner (Fig. 5C). Similar inhibitory effects on NO release and activation-induced cell death were observed with E-64 and LLnL (data not shown).

Next, we examined whether AEBSF, E-64, or LLnL regulate glioma cell death mediated by microglia MCM. The serine protease inhibitor, AEBSF, had little effect on MCM-induced cell death (Fig. 5D). Additionally, LLnL exerted no significant influence (data not shown). However, treatment with E64, a general cysteine protease inhibitor, which also acts on lysosomal cysteine cathepsins [32], resulted in suppression of MCM-

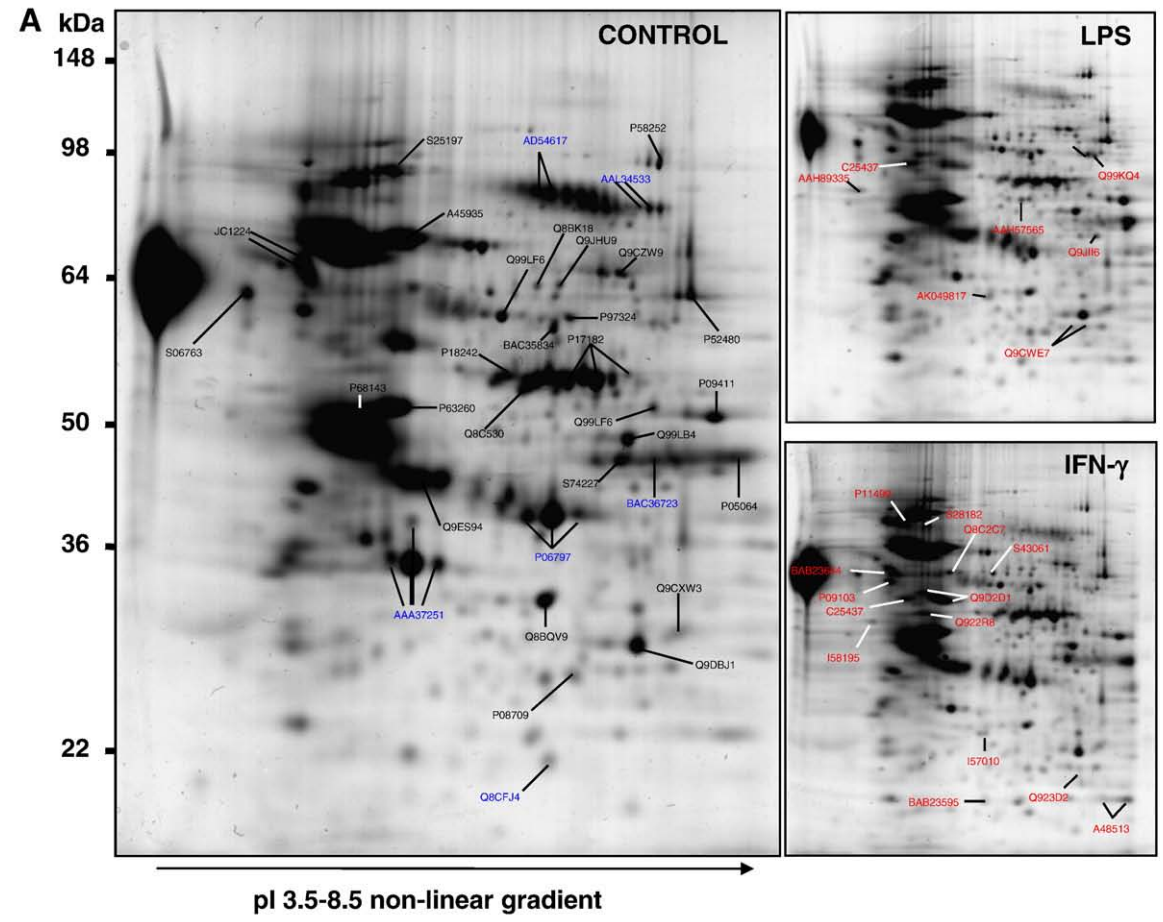
A
kDa
148
98
64
50
36
22
CONTROL
LPS
IFN-γ
S25197
AD54617
P58252
AAL34533
A45935
JC1224
Q8BK18
Q9JHU9
Q9CZW9
Q99LF6
S06763
P97324
P52480
BAC35634
P17182
P18242
P68143
P63260
Q8C530
P09411
Q99LF6
Q99LB4
S74227
BAC36723
P05064
Q9ES94
P06797
AAA37251
Q9CXW3
Q8BQV9
Q9DBJ1
P08709
Q8CFJ4
C25437
AAH89335
Q99KQ4
AAH57565
Q9JII6
AK049817
Q9CWE7
P11499
S28182
Q8C2C7
S43061
BAB23664
P09103
C25437
Q9D2D1
Q922R8
I58195
I57010
BAB23595
Q923D2
A48513
pI 3.5-8.5 non-linear gradient

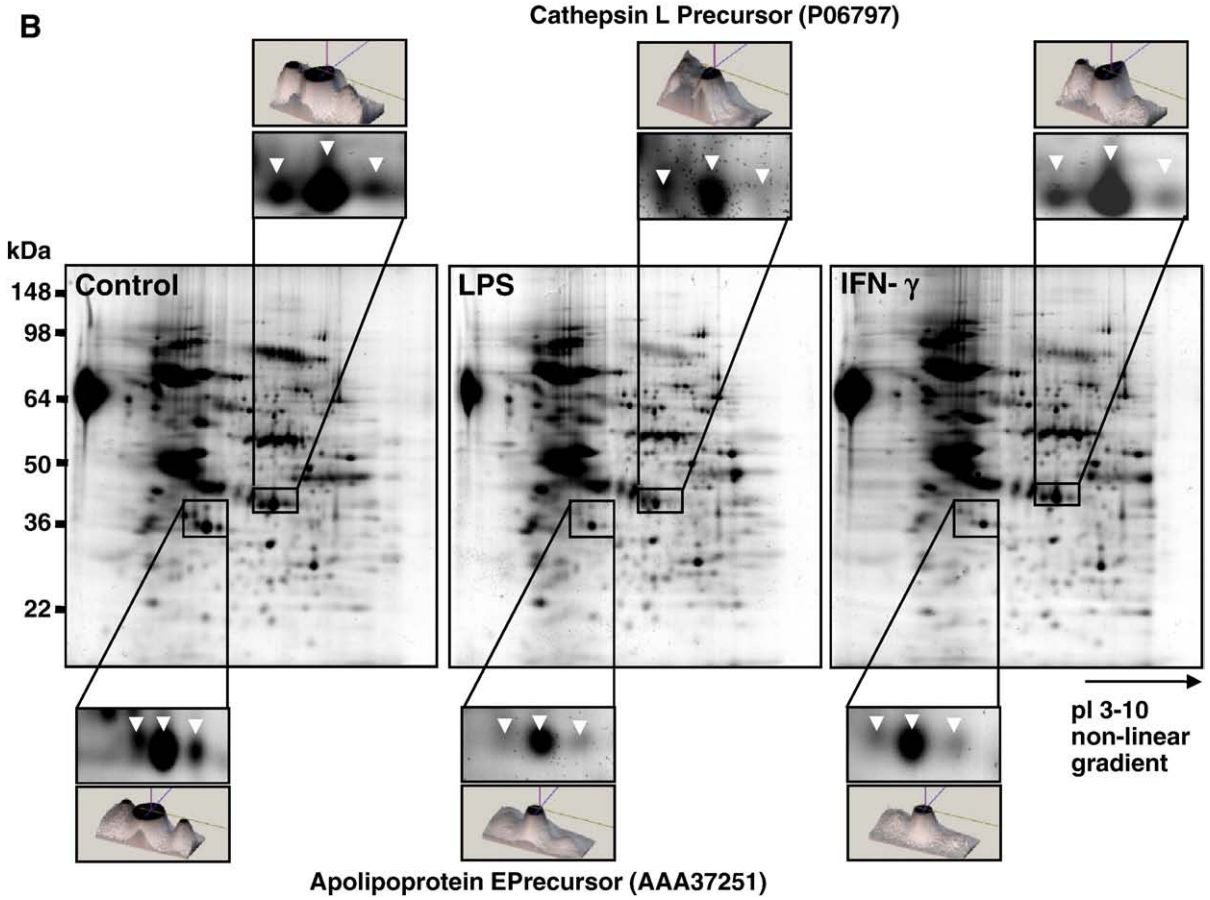
B
Cathepsin L Precursor (P06797)
kDa
148
98
64
50
36
22
Control
LPS
IFN- γ
pI 3-10
non-linear
gradient
Apolipoprotein EPrecursor (AAA37251)

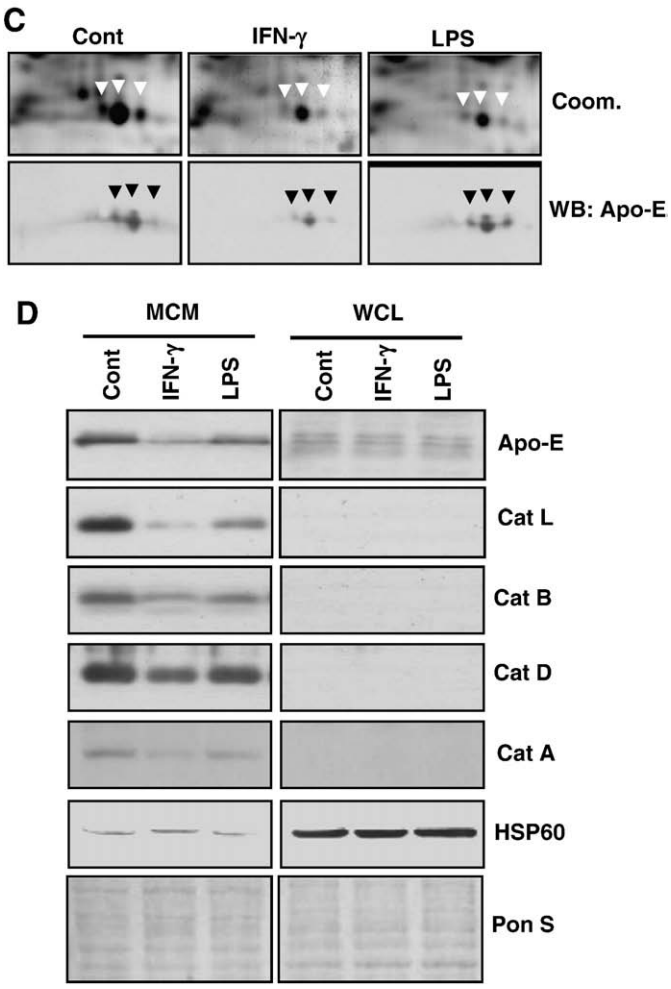


**Fig. 4.** Reference 2-D maps of MCM prepared from control and LPS- or IFN-γ-activated mouse BV2 microglia and validation of proteins displaying altered secretion patterns in the presence of LPS, or IFN-γ. Images were scanned at a resolution of 300 DPI. Proteins (250 μg) were separated on a nonlinear pH 3–10 IPG strip, followed by 10% SDS–PAGE. Approximately 400 modified Coomassie-stained protein spots were detected with the ImageMaster™ software program on each gel. (A) Typical patterns of 2-D gels of secretory proteins. Up- or down-regulated proteins in MCM of BV2 cells treated with LPS or IFN-γ were selected with ImageMaster ™. Proteins were excised from the main gel and digested with trypsin, and peptides were analyzed by MALDI-MS. Proteins were identified based on peptide mass. Swiss-Prot accession numbers of normal and up- and down-regulated proteins were labeled in black, red, and blue, respectively. (B) Enlarged partial images of gels containing apolipoprotein E (AAA37251) and cathepsin L (P06797) precursor protein spots. Enlarged 2- and 3-dimensional images disclose down-regulation of these two proteins in MCM of LPS- or IFN-γ-treated BV2. (C) BV2 cells were left untreated (cont) or stimulated with 10 ng/ml of LPS or 20 U/ml IFN-γ for 24 h. Coomassie blue staining (coom.) and Western blotting (WB) of apolipoprotein E proteins after 2-D gel electrophoresis of BV2 secretory proteins. (D) Western blotting of secretory proteins (MCM) and whole cell lysates (WCL). BV2 cells were left untreated (cont) or stimulated with 10 ng/ml LPS or 20 U/ml IFN-γ for 24 h. An aliquot of protein (20 μg per lane) was separated in 10% SDS–PAGE and subjected to Western blotting for apolipoprotein E (ApoE) and cathepsin (Cat) protease family (A, B, D, and L) proteins. Ponceau S (Pon S)-stained protein blots reveal equal protein loading per lane. Shown data are representative of at least three separate experiments.

induced glioma cell death (Fig. 5D). Unfortunately, this analysis was hampered since E-64 itself displayed some toxicity, particularly at higher concentrations (>15% cell death at doses higher than 5 μM). Nevertheless, E-64 protected glioma cells from MCM-induced death.

### *3.6. The cathepsin B inhibitor, CA-074me, suppresses MCM-induced glioma cell death*

We next addressed whether microglia-secreted cathepsins are essential in stimulating cytotoxicity in glioma cells. Neither microglial activation nor MCM-mediated cell death was influenced by cathepsin B, L, and S specific inhibitors, Z-FG-NHO-BzME, and Z-FG-NHO-Bz (data not shown). Moreover, immunodepletion of cathepsins with specific antibodies for cathepsin A, B, D, L, and K did not abolish the cytotoxic effects of MCM on CRT-MG glioma cells (data not shown). Strikingly, inhibition of the enzymatic activity of cathepsin B by CA-074me to MCM demonstrated inhibition of glioma cell death (Fig. 6A and B). CA-074me did not influence astrocyte either alone or in combination with MCM (Fig. 6C). Importantly, general cysteine protease inhibitor, E-64, together with CA-074me displayed an additive effect on protection against MCM-induced glioma cell death (data not shown), indicating that other cysteine proteinases also can be involved in cytotoxicity. Direct treatment of CRT-MG with cathepsin B caused a decrease in cell survival (by ~20%) (Fig. 6D). These results strongly suggest that cathepsin B is an important mediator of MCM-induced glioma cell death.

## 4. Discussion

Since microglia produce and secrete various molecules in both the resting and activated states, microglia-mediated responses to brain tumors may be broadly influenced by secreted soluble factors. The microglial soluble factor(s) involved in glioma proliferation or death remain to be identified. In this report, we show that substance(s) released by microglia induce apoptosis of astrocytic glioma cells. Significantly, the cytotoxic effects of MCM were specific for astrocytic glioma cells, since primary cultured astrocyte survival was not

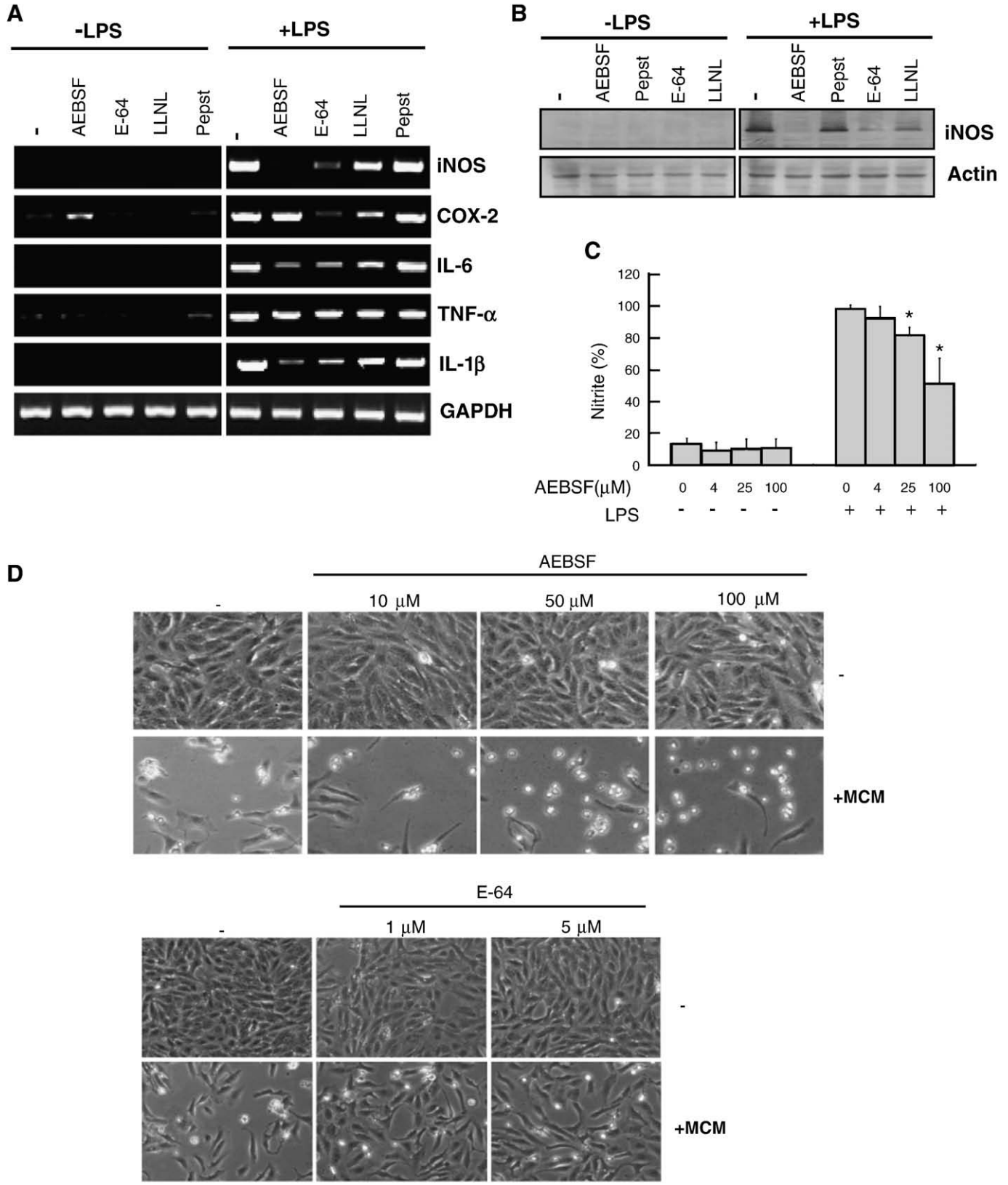


**Fig. 5.** Effects of various protease inhibitors on microglia activation and MCM-induced glioma cell death. BV2 microglia cells were left untreated or stimulated with LPS (100 ng/ml) in the presence of AEBSF (100 μM for A and B), E-64 (10 μM), LLnL (2.5 μM), and pepstatin A (pepst) (10 μM) for 24 h. (A) Total RNA was extracted and mRNA levels were measured by RT-PCR using specific primers. (B) Western blotting of total cell lysates (20 μg of protein sample per lane) subjected to 10% SDS–PAGE. (C) BV2 cells were pretreated with varying concentrations of AEBSF, and nitrite levels were determined. (D) CRT-MG glioma cells were incubated with MCM prepared from BV2 with or without the indicated concentrations of AEBSF or E-64. At 72 h, cell status and morphological changes in CRT-MG glioma cells were observed under a light microscope. Data in (A), (B), and (D) are representative of four independent experiments. Data presented in (C) are means ± SEM of three independent experiments. The asterisk represents significant reduction compare to cells stimulated with LPS alone.

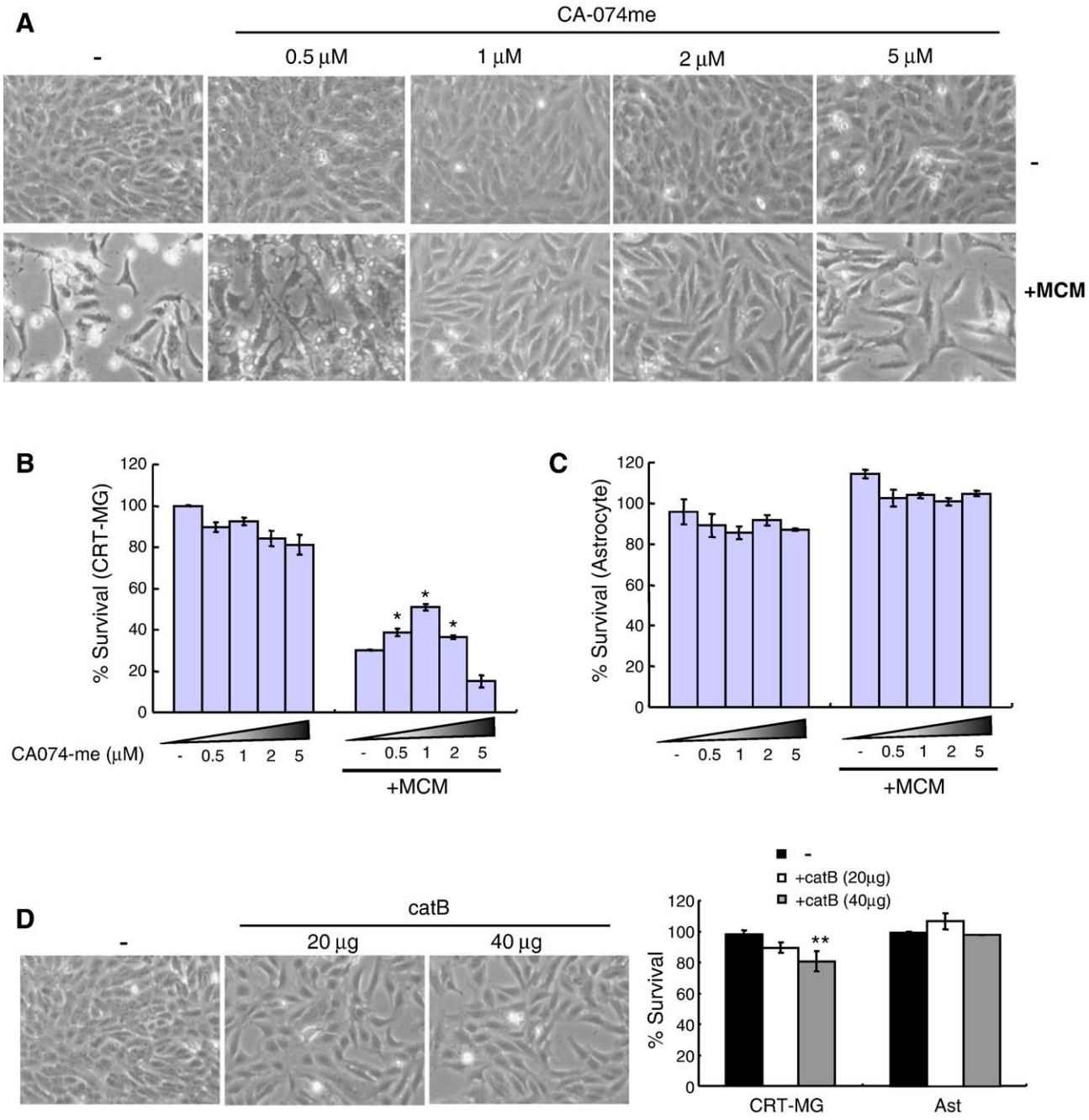


**Fig. 6.** Effects of CA-074me on MCM-induced glioma cell death and influence of cathepsin B on glioma cell proliferation. (A) MCM with or without the indicated concentrations of CA-074me was incubated with CRT-MG glioma cells for 72 h. The morphology of CRT-MG glioma cells was observed under a light microscope. (B) Survival rates of CRT-MG glioma cells and (C) primary astrocyte cells were determined with the MTT assay. (D) The CRT-MG glioma cell line was directly treated with exogenous cathepsin B for 72 h. Cell morphology was observed under a light microscope (left panel) and cell survival rates were determined with the MTT assay (right panel). Data in (A) and (D) are representative of three independent experiments. Data presented in (B) and (C) are means ± SEM of three independent experiments. * Indicates values significantly increased compared to cultures incubated with MCM. ** Indicates values significantly different from untreated control cultures.

influenced. In fact, MCM induced mild, but consistent proliferation of astrocytes (data not shown). This selective cytotoxic effect was enhanced upon microglial activation.

The viability of glioma cells was remarkably decreased in the presence of SIN-1 at concentrations of 400–1000 μM, which usually releases about 20–40 μM nitrite into culture medium at 72 h. In contrast, astrocytes were resistant to SIN-1, even at 1000 μM. The data suggest that activated microglia selectively induce glioma cell apoptosis by activating iNOS and subsequent release of NO. Furthermore, we also found that combined treatment with IL-1β, TNF-α, and IL-6 significantly potentiated SIN-1-induced cytotoxicity. Thus, our report provides new information, demonstrating that microglial-secreted NO acts in concert with proinflammatory cytokines to play an important role in regulating tumor growth.

NO effect was insufficient to explain glioma cell death by MCM. MCM induced significant cell death, despite the presence of very low levels of NO. Furthermore, inclusion of NOS inhibitors into microglia culture led to significant suppression of glioma cell death mediated by activated MCM, but not by MCM. Thus, it is likely that NO in the activated MCM is the principal cytotoxic mediator of glioma, while cathepsin B released by microglia in the resting state may be critical in the induction of glioma cytotoxicity.

One issue for consideration is that depletion of nutrients or energy sources in the culture medium elicits apoptosis of glioma cells. To eliminate this possibility, we added pyruvate (2 mM) to the culture medium as an energy source, which did not affect glioma apoptosis (data not shown). In addition, conditioned culture medium prepared similarly from other cells (rat2 mouse fibroblasts or A549 lung adenocarcinoma cells) elicited no significant effects on glioma cell survival or proliferation (data not shown). Furthermore, conditioned media from rat2 mouse fibroblasts or A549 lung adenocarcinoma cells stimulated with LPS or IFN-γ did not induce any influences on glioma cell survival/proliferation (data not shown). Nonetheless, there is no evidence to rule out the possibility of depletion of critical factor(s) required for glioma survival in MCM.

To identify the proteins secreted by microglia and compare their expression patterns in the unstimulated and stimulated states, we established 2-D maps of BV2 microglia secretory proteins obtained from either control MCM or MCM stimulated by LPS or IFN-γ. Notably, apolipoprotein E (ApoE) and cathepsin proteases displayed the most marked alterations in the presence of LPS and IFN-γ. Our finding that ApoE is down-regulated in BV2 MCM treated with LPS and IFN-γ is consistent with previous reports [33,34]. Moreover, the low level of endogenous ApoE in non-treated and LPS- and IFN-γ-treated cells suggests that either secretion or protein expression of ApoE is regulated. Since the mRNA level of ApoE was not changed by LPS or IFN-γ, we hypothesize that the secretion phase or protein stability is regulated. Immunodepletion of ApoE using specific antibodies did not influence MCM-mediated apoptosis of glioma (data not shown). In addition, exogenous ApoE4 did not induce phenotypic or cytotoxic effects on glioma cells (data not shown), ruling out its direct involvement in glioma cell survival. While the effects of other isoforms of ApoE (ApoE2 and ApoE3) remain to be established, current data suggest that the protein does not have a critical function in microglia-mediated cytotoxicity of glioma cells.

In our experiments, secretion of several lysosomal cathepsin proteases (A, B, D, and L) was suppressed by LPS or IFN-γ. In contrast to our findings, up-regulated extracellular accumulation of cathepsin L has been reported in IFN-γ-treated macrophages and LPS-activated dendritic cells [35]. In addition, treatment of human U-937 monocytes and macrophages with IFN-γ leads to an increase in the activity and content of cathepsins B and L [35,36]. These inconsistent results may reflect the characteristics of microglia response in neuroinflammation processes and various neuronal diseases. Up-regulated extracellular accumulation of cathepsin D has been also reported in LPS/IFN-γ-treated BV2 cells [37]. While the reason for the discrepancy in response between LPS or IFN-γ and LPS plus IFN-γ for cathepsin D release remains to be elucidated, one possibility includes that combinatory signals from LPS and IFN-γ are required for increased expression of cathepsin D. Among the cathepsin proteins, the importance of cathepsin B in inflammation-related cytotoxicity has been extensively examined. E-64 and CA-074me [32,38], inhibitors for cathepsin B, significantly suppressed glioma apoptosis. In view of these results, we propose that cathepsin B is a critical factor in MCM-mediated glioma death. The purified cathepsin B induced significant but relatively mild cytotoxic effect on glioma (~20% reduction in cell viability). This may be due to the relatively weak biological effect of purified cathepsin B compared to endogenous proteins or the potential presence of a critical regulator or cofactor of cathepsin B in MCM. Accumulating knowledge on proteolytic events and subsequent effects in brain inflammation and cell death mediated by microglial proteases will not only contribute to a better understanding of the role of microglial-secreted proteins in the CNS but also aid in the development of protease inhibitors as novel neuroprotective or neuro-immunoregulatory agents. Given the dynamic regulation of microglia-secreted proteins, characterization of the functions of other cathepsin proteins (A, D, K, L, and Z) in brain physiology and pathology is essential. It has been shown that microglial produced MMP-3 or -9 are involved in microglial activation [39,40]. While the roles of MMPs in glioma invasion are described in many reports, few studies focused on apoptotic effects of MMPs to glioma cells. Our proteomic data did not show any evidences for (changed) expression of MMPs in BV2 conditioned medium.

To date, 2-D-based proteome mapping has been limited to the detection of large proteins or relatively high concentrations of proteins. Thus, low abundance proteins have undoubtedly been overlooked due to the inadequate sensitivity of Coomassie blue staining. Future laboratory analyses will employ fluorescent stains or isotope labeling, which should allow the efficient analysis of less abundant proteins.

In conclusion, our results support the idea that microglia play an active role in the regulation of tumor cell death by local secretion of NO and cathepsin B. It is currently unclear how exogenous cathepsin B initiates or propagates proapoptotic signals. One possibility includes that cathepsin B could nonspecifically degrade important cell surface proteins, thereby causing the cell to initiate apoptosis. Alternatively, cathepsin B could cleave extracellular matrix proteins, which are important for cell survival, thereby causing apoptosis. We expect that future studies aimed at identifying the downstream targets of cathepsin B effects will contribute to the understanding of microglial produced proteases in pathogenesis of brain tumor. Because microglial secretion of these molecules is dynamically regulated by stimulation with LPS or IFN-γ, the modulation of microglial activation may contribute to the control of brain neoplasms.

## Acknowledgements

This study was supported by a grant of the Korea Healthcare technology R&D project, Ministry for Health, Welfare & Family Affairs, Republic of Korea (A080438).

## Appendix A. Supplementary data

Supplementary data associated with this article can be found, in the online version, at doi:10.1016/j.bbamcr.2009.08.011.

## References

[1] M. Shinonaga, C.C. Chang, N. Suzuki, M. Sato, T. Kuwabara, Immunohistological evaluation of macrophage infiltrates in brain tumors. Correlation with peritumoral edema, J. Neurosurg. 68 (1988) 259–265.
[2] W. Roggendorf, S. Strupp, W. Paulus, Distribution and characterization of microglia/macrophages in human brain tumors, Acta Neuropathol. (Berl) 92 (1996) 288–293.
[3] B. Badie, J.M. Schartner, Flow cytometric characterization of tumor-associated macrophages in experimental gliomas, Neurosurgery 46 (2000) 957–961 discussion 961-952.
[4] S.F. Hussain, D. Yang, D. Suki, K. Aldape, E. Grimm, A.B. Heimberger, The role of human glioma-infiltrating microglia/macrophages in mediating antitumor immune responses, Neuro. Oncol. 8 (2006) 261–279.
[5] B. Badie, J. Schartner, Role of microglia in glioma biology, Microsc. Res. Tech. 54 (2001) 106–113.
[6] M.B. Graeber, B.W. Scheithauer, G.W. Kreutzberg, Microglia in brain tumors, GLIA 40 (2002) 252–259.
[7] A.A. Rosales, R.S. Roque, Microglia-derived cytotoxic factors. Part I. Inhibition of tumor cell growth in vitro, Brain Res. 748 (1997) 195–204.
[8] J.T. Groves, Peroxynitrite: reactive, invasive and enigmatic, Curr. Opin. Chem. Biol. 3 (1999) 226–235.
[9] W.A. Pryor, G.L. Squadrito, The chemistry of peroxynitrite: a product from the reaction of nitric oxide with superoxide, Am. J. Physiol. 268 (1995) L699–L722.
[10] T.K. Makar, M. Nedergaard, A. Preuss, A.S. Gelbard, A.S. Perumal, A.J. Cooper, Vitamin E, ascorbate, glutathione, glutathione disulfide, and enzymes of glutathione metabolism in cultures of chick astrocytes and neurons: evidence that astrocytes play an important role in antioxidative processes in the brain, J. Neurochem. 62 (1994) 45–53.
[11] N. Amin, B. Pearce, Peroxynitrite-induced toxicity in cultured astrocytes, Brain Res. 773 (1997) 227–230.
[12] S. Qiao, W. Li, R. Tsubouchi, M. Haneda, K. Murakami, M. Yoshino, Involvement of peroxynitrite in capsaicin-induced apoptosis of C6 glioma cells, Neurosci. Res. 51 (2005) 175–183.
[13] M. Pehar, L. Martinez-Palma, H. Peluffo, A. Kamaid, P. Cassina, L. Barbeito, Peroxynitrite-induced cytotoxicity in cultured astrocytes is associated with

morphological changes and increased nitrotyrosine immunoreactivity, Neurotox. Res. 4 (2002) 87–93.
[14] Y.C. Kang, P.K. Kim, B.M. Choi, et al., Regulation of programmed cell death in neuronal cells by nitric oxide, In Vivo 18 (2004) 367–376.
[15] P.K. Kim, Y.G. Kwon, H.T. Chung, Y.M. Kim, Regulation of caspases by nitric oxide, Ann. N.Y. Acad. Sci. 962 (2002) 42–52.
[16] S.J. Lee, K.M. Kim, S. Namkoong, et al., Nitric oxide inhibition of homocysteine-induced human endothelial cell apoptosis by down-regulation of p53-dependent Noxa expression through the formation of *S*-nitrosohomocysteine, J. Biol. Chem. 280 (2005) 5781–5788.
[17] E. Thouvenot, M. Lafon-Cazal, E. Demettre, P. Jouin, J. Bockaert, P. Marin, The proteomic analysis of mouse choroid plexus secretome reveals a high protein secretion capacity of choroidal epithelial cells, Proteomics 6 (2006) 5941–5952.
[18] A. Dupont, D. Corseaux, O. Dekeyzer, et al., The proteome and secretome of human arterial smooth muscle cells, Proteomics 5 (2005) 585–596.
[19] L. Gan, S. Ye, A. Chu, et al., Identification of cathepsin B as a mediator of neuronal death induced by Abeta-activated microglial cells using a functional genomics approach, J. Biol. Chem. 279 (2004) 5565–5572.
[20] J. Gray, M.M. Haran, K. Schneider, et al., Evidence that inhibition of cathepsin-B contributes to the neuroprotective properties of caspase inhibitor Tyr-Val-Ala-Asp-chloromethyl ketone, J. Biol. Chem. 276 (2001) 32750–32755.
[21] R. Berti, A.J. Williams, J.R. Moffett, et al., Quantitative real-time RT-PCR analysis of inflammatory gene expression associated with ischemia–reperfusion brain injury, J. Cereb. Blood Flow Metab. 22 (2002) 1068–1079.
[22] W.K. Kim, S.Y. Hwang, E.S. Oh, H.Z. Piao, K.W. Kim, I.O. Han, TGF-beta1 represses activation and resultant death of microglia via inhibition of phosphatidylinositol 3-kinase activity, J. Immunol. 172 (2004) 7015–7023.
[23] H.S. Kim, S.Y. Whang, M.S. Woo, J.S. Park, W.K. Kim, I.O. Han, Sodium butyrate suppresses interferon-gamma-, but not lipopolysaccharide-mediated induction of nitric oxide and tumor necrosis factor-alpha in microglia, J. Neuroimmunol. 151 (2004) 85–93.
[24] S. Goswami, A. Gupta, S.K. Sharma, Interleukin-6-mediated autocrine growth promotion in human glioblastoma multiforme cell line U87MG, J. Neurochem. 71 (1998) 1837–1845.
[25] C. Choi, O. Kutsch, J. Park, T. Zhou, D.W. Seol, E.N. Benveniste, Tumor necrosis factor-related apoptosis-inducing ligand induces caspase-dependent interleukin-8 expression and apoptosis in human astroglioma cells, Mol. Cell. Biol. 22 (2002) 724–736.
[26] M.A. Hotz, J. Gong, F. Traganos, Z. Darzynkiewicz, Flow cytometric detection of apoptosis: comparison of the assays of in situ DNA degradation and chromatin changes, Cytometry 15 (1994) 237–244.
[27] Z. Darzynkiewicz, S. Bruno, G. Del Bino, et al., Features of apoptotic cells measured by flow cytometry, Cytometry 13 (1992) 795–808.
[28] Y.K. Shin, B.C. Yoo, H.J. Chang, et al., Down-regulation of mitochondrial F1F0-ATP synthase in human colon cancer cells with induced 5-fluorouracil resistance, Cancer Res. 65 (2005) 3162–3170.
[29] Y. Lee da, Y.J. Oh, B.K. Jin, Thrombin-activated microglia contribute to death of dopaminergic neurons in rat mesencephalic cultures: dual roles of mitogen-activated protein kinase signaling pathways, Glia 51 (2005) 98–110.
[30] M. Kelm, R. Dahmann, D. Wink, M. Feelisch, The nitric oxide/superoxide assay. Insights into the biological chemistry of the NO/O-2. interaction, J. Biol. Chem. 272 (1997) 9922–9932.
[31] X. Yang, R.G. Schnellmann, Proteinases in renal cell death, J. Toxicol. Environ. Health 48 (1996) 319–332.
[32] K. Matsumoto, K. Mizoue, K. Kitamura, W.C. Tse, C.P. Huber, T. Ishida, Structural basis of inhibition of cysteine proteases by E-64 and its derivatives, Biopolymers 51 (1999) 99–107.
[33] R.L. Oropeza, H. Wekerle, Z. Werb, Expression of apolipoprotein E by mouse brain astrocytes and its modulation by interferon-gamma, Brain Res. 410 (1987) 45–51.
[34] K. Brand, N. Mackman, L.K. Curtiss, Interferon-gamma inhibits macrophage apolipoprotein E production by posttranslational mechanisms, J. Clin. Invest. 91 (1993) 2031–2039.
[35] E. Fiebiger, R. Maehr, J. Villadangos, et al., Invariant chain controls the activity of extracellular cathepsin L, J. Exp. Med. 196 (2002) 1263–1269.
[36] T.T. Lah, M. Hawley, K.L. Rock, A.L. Goldberg, Gamma-interferon causes a selective induction of the lysosomal proteases, cathepsins B and L, in macrophages, FEBS Lett. 363 (1995) 85–89.
[37] S. Kim, J. Ock, A.K. Kim, et al., Neurotoxicity of microglial cathepsin D revealed by secretome analysis, J. Neurochem. 103 (2007) 2640–2650.
[38] D.T. Jane, L.C. Morvay, F. Allen, B.F. Sloane, M.J. Dufresne, Selective inhibition of cathepsin B with cell-permeable CA074Me negatively affects L6 rat myoblast differentiation, Biochem. Cell. Biol. 80 (2002) 457–465.
[39] M.S. Woo, J.S. Park, I.Y. Choi, W.K. Kim, H.S. Kim, Inhibition of MMP-3 or -9 suppresses lipopolysaccharide-induced expression of proinflammatory cytokines and iNOS in microglia, J. Neurochem. 106 (2008) 770–780.
[40] Y.S. Kim, S.S. Kim, J.J. Cho, et al., Matrix metalloproteinase-3: a novel signaling proteinase from apoptotic neuronal cells that activates microglia, J. Neurosci. 25 (2005) 3701–3711.